1. SCIENTIFIC GOALS AND OBJECTIVES

A radio interferometer array in space providing high dynamic range images with arcminute angular resolution at frequencies below the ionospheric cutoff will open new vistas in solar, terrestrial, galactic, and extragalactic astrophysics. It will be able to produce the first sensitive, high angular resolution survey of the entire sky at frequencies between 0.03 and 30 MHz. Basic physics predicts that the radio sky will look entirely different at frequencies below ~30 MHz due to the dominance of new emission and absorption processes such that opening this last, unexplored part of the electromagnetic spectrum will provide a fundamentally new view of the universe. Just as importantly, a low frequency space array will be able to image and track transient disturbances in the solar corona and interplanetary medium — a new capability which is critical for understanding many aspects of solar-terrestrial interaction and space weather.

1.1 INTRODUCTION

A low frequency space array (LFSA) will produce the first sensitive, high resolution radio images of the entire sky at frequencies below 30 MHz — a region of the spectrum that remains unexplored with high angular resolution. Many physical processes involved in the emission and absorption of radiation are only observable at low radio frequencies. For example, the coherent emission associated with electron cyclotron masers, as seen from the giant planets, Earth (Auroral Kilometric Radiation), and several nearby stars, is not only expected to occur and be detectable elsewhere in the Galaxy but to be ubiquitous. Incoherent synchrotron radiation from fossil radio galaxies will be detectable by a LFSA, revealing the frequency and duration of past epochs of nuclear activity. It is also likely that unexpected objects and processes will be discovered by a LFSA. Indeed, one of the cornerstones of such a space array is its very high potential for discovery.

A LFSA will also produce the first low frequency, high resolution radio images of the solar corona and interplanetary disturbances such as shocks driven by coronal mass ejections (CMEs). To image and track these solar induced disturbances from the vicinity of the sun all the way to 1 AU requires observing frequencies from tens of kHz to tens of MHz. Since Earth's ionosphere severely limits radio interferometry from the ground at frequencies below ~30 MHz, these measurements must be made from space. A low frequency imaging interferometer will operate from 0.03 to 30.0 MHz.

CMEs interacting with Earth's magnetosphere can result in geomagnetic storms which are capable of damaging satellite and electric utility systems and disrupting communications and GPS navigation services. Solar disturbances can also pose a threat to astronauts. One of the space-weather goals of a LFSA is accurate prediction, days in advance, of the arrival of CMEs at Earth. In addition, a LFSA will image Earth's magnetospheric response to such solar disturbances, providing a unique global view of the magnetosphere from the outside.

Because the solar and extra-solar-system astrophysics programs are traditionally somewhat separate areas of study within the astronomical community, we discuss their science goals separately. However, it should be kept in mind that a LFSA will simultaneously address key issues in both the astrophysics and solar/space physics areas with no significant increase in cost or compromise in array design.

In astrophysics, a LFSA will address:

- *galaxy evolution* — detection of fossil radio galaxies and very-high-redshift radio galaxies, and cosmic ray diffusion times and magnetic field distributions in our Galaxy and other galaxies.
- *life cycles of matter* — distribution of diffuse ionized hydrogen in the interstellar medium, energy transport via interstellar plasma turbulence, origin of cosmic ray electrons, and the detection of old galactic supernova and γ-ray burst remnants.
- *Discovery of new phenomena and tests of physical theories* — new sources of coherent radio emission, pulsar emission regions, shock acceleration, physics of electrically charged dusty plasmas, new classes of very steep spectrum objects not seen at higher frequencies, and halo emission from clusters of galaxies.

In solar/space physics, a LFSA will address:

- *solar variability* — physics of solar transient disturbances, the evolution of coronal and solar wind structures, and interactions of plasma and magnetic field topology.
- *solar-terrestrial interaction* — solar interactions with Earth's magnetosphere, geomagnetic storms, and space weather.
- *space weather forecasting* — forecast the arrival of coronal mass ejections.

The fundamental technique of a LFSA is aperture synthesis, in which interferometric data from a large number of baseline lengths and orientations are combined to produce images with an angular resolution comparable to that of a single aperture the size of the entire interferometer array. This is the basis of ground-based arrays such as the VLA and VLBA and the VSOP space VLBI mission, and results in many orders of magnitude improvement in angular resolution. The concept for opening the low frequency window from space was endorsed by the radio astronomy panel of the Bahcall committee, which recommended "...establishing a program of space radio astrophysics during the next decade leading to the establishment of a LFSA, a free flying hectometer wavelength synthesis array for high resolution imaging, operating below the ionospheric cutoff frequency."

A low frequency imaging interferometer would consist of a large number (>12) of identical small satellites with dipole antennas and low frequency radio receivers, distributed in a spherical array ~100 km in diameter. The array placement is under discussion, but a nearly circular orbit ~10^6 km from Earth has been found to be dynamically stable with well understood properties and far enough from Earth to avoid terrestrial interference. The size of the array is determined by a fundamental limit to angular resolution created by the scattering of radio waves in the interstellar and interplanetary media. However, the scattering limit is a strong function of direction and observing frequency. To allow for this, it should be possible to vary the size of the array during its lifetime to increase or decrease the maximum angular resolution if desired.

Figure 1 shows the angular resolution of a LFSA compared to several ground-based radio arrays and to the angular broadening caused by interstellar scattering at intermediate galactic latitudes. The shaded region is inaccessible from the ground with high angular resolution.

Figure 1 — Angular resolution of A low frequency array as a function of observing frequency.

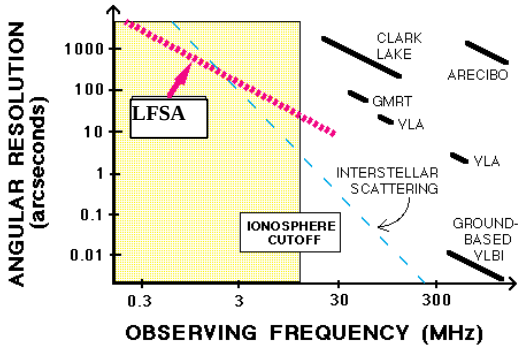

Figure 1 — Angular resolution of a low frequency array as a function of observing frequency.

Figure 2 and Table 1 indicate how the number of satellites, the array orbit, and other array design issues are derived.

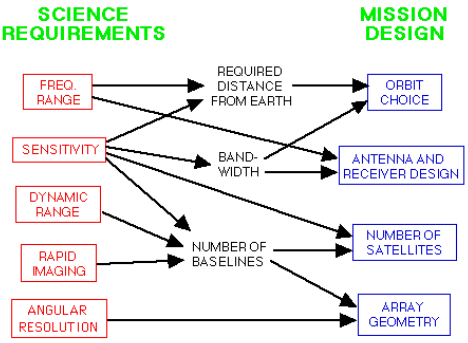

Figure 2 — A LFSA design is derived from observational capabilities needed to meet the science objectives.

Science Requirement	Array Parameters
Observe below Earth's ionosphere cutoff freq.	Freq. range: 30 MHz to 30 kHz (local plasma freq.)
Angular resolution of ~1 arcminute at 10 MHz.	~100 km maximum array baseline length
Good instantaneous aperture plane sampling	>66 simultaneous baselines (>12 array satellites)
Sensitivity at 10 MHz of 50 Jy in less than 1 hour	Up to 125 kHz bandwidth, crossed dipole antennas
Dynamic range ~1000 for fields far from the sun	3-D array geometry, dense aperture plane sampling

Table 1 — Detailed observing requirements.

1.2 LOW FREQUENCY ASTROPHYSICS

Multi-frequency, all-sky radio images produced by a LFSA will allow the spectra of known galactic and extragalactic objects to be extended to much lower frequencies. This will provide unique information on how galaxies evolve, matter in extreme conditions, and on the life cycles of matter in the universe. In addition, objects unseen at higher frequencies are almost certain to be found, resulting in the discovery of new phenomena..

1.2.1 Introduction

In an ingenious analysis, Harwit (1984) concluded that we have discovered approximately one third of the phenomena in the universe. All but 4 of the 43 phenomena in his study were discovered in the eight decade range between 3 x 10^7 and 3 x 10^{15} Hz. How many other phenomena remain to be discovered in what is arguably the last frontier in the electromagnetic spectrum, the three decades from 30 kHz to 30 MHz? A LFSA will explore this wide range with high angular resolution and sensitivity, which can only be done from space: Below 30 MHz very strong terrestrial radio interference and ionospheric absorption and refraction make the imaging of cosmic radio sources extremely difficult. Below ~10 MHz the ionosphere is opaque almost all the time almost everywhere on Earth. Even at the best ground-based locations astronomical observations are impossible below ~3 MHz. Between 3 MHz and the interplanetary plasma cutoff near 30 kHz ($\lambda = 10$ km) there have been some observations from individual spacecraft, but with very poor angular resolution. A low frequency imaging interferometer will revolutionize astronomical observations at low frequencies. Two of Harwit's conclusions are particularly pertinent: "Many discoveries...depended on equipment less than five years old" (i.e., new discoveries require new observing capabilities) and "About half the discoveries made have been serendipitous."

In addition to its very high potential for discovery, a LFSA will address several key issues in astrophysics, including: 1) understanding the evolution of galaxies, 2) the exchange of matter and energy among stars and the interstellar medium, and 3) testing physical theories and revealing new phenomena. In each case, the key contribution of a LFSA will be unprecedented angular resolution and sensitivity in a nearly unexplored frequency range.

Figure 3 illustrates the dramatic gains to be made by going from approximately one steradian angular resolution (a single spacecraft observing at a few MHz — the current state of the art) to the arcminute angular resolution provided by a LFSA at a few MHz.

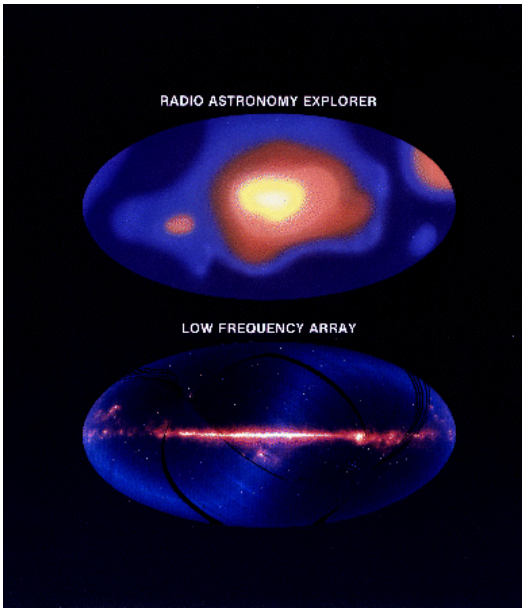

Figure 3 — All-sky image from single-spacecraft Radio Astronomy Explorer (RAE) mission (top) compared with simulated (from IRAS data) all-sky image from a LFSA (bottom).

This gain in resolution and sensitivity will enable a LFSA to detect and resolve individual objects anywhere on the sky and determine their low frequency spectra from imaging at multiple frequencies. As a result, a LFSA will open up an entirely new regime of astrophysical investigation. Among the specific astrophysics objectives of a LFSA are:

The evolution of galaxies

- Search for "fossil" radio galaxies to obtain information on the frequency and duration

of the active phases of galactic nuclei, and on the intergalactic magnetic field.
- Search for very high redshift radio galaxies, which typically have steeper spectra than closer radio galaxies.
- Determine cosmic ray diffusion times away from galactic disks.

Life cycles of matter in the universe

- Accurately map diffuse interstellar ionized hydrogen, the last major component of the interstellar medium whose distribution is not currently well determined.
- Study the origin & transport of turbulence in the interstellar medium; constrain models for the dissipation of turbulent energy.
- Rigorously test the hypothesis that cosmic ray electrons originate in galactic super-nova remnants.
- Map the 3-dimensional distribution of galactic low energy cosmic ray electrons to improve our understanding of cosmic ray transport and escape.

Discovery of new phenomena & tests of physical theories

- Search for expected new sources of coherent radiation and determine the conditions in extreme plasma environments, including emission regions of millisecond pulsars.
- Test the diffusive shock acceleration model for the origin of cosmic rays; understand acceleration & energy loss processes in supernova remnants.
- Search for new sources of galactic non-thermal emission in supernova remnants, HI supershells (possible γ-ray burst remnants), large-scale ionized filaments, and the "galactic center fountain."
- Test the hypothesis that diffuse x-ray and UV radiation from galaxy clusters is produced by inverse-Compton scattering of microwave photons by the relativistic electrons responsible for steep spectrum radio halo emission.
- Test the theory of coherent scattering of long-wavelength radio radiation by electrically charged dusty plasmas.
- Search for cyclotron emission from giant planets orbiting nearby stars.

The following Sections cover these LFSA science goals in more detail.

1.2.2 How do galaxies evolve?

Evidence of previous galactic activity

Are there significant numbers of galaxies which had active nuclei in the distant past but are now quiescent? The discovery of a significant number of "fossil" radio galaxies would provide important new constraints on galaxy evolution and specifically on the frequency and lifetime of active phases. A LFSA *will search for fossil radio components associated with presently radio quiet galaxies (e.g., Goss, et al., 1987; Cordey, 1987; Reynolds and Begelman 1997) as well as presently active galaxies to determine how often and for how long galaxies were active in the past.* Information on early epochs of galactic activity and its duration can help constrain models for the evolution of massive black holes in galactic nuclei. The long radiative lifetimes of electrons at low frequencies will preserve evidence of early phases of activity in galaxies which are too faint at higher frequencies to be included in existing radio catalogs. For example, a synchrotron source with an initial spectral index of -0.7 and 10^{-5} G magnetic field will have a spectral index of -2 above 3 MHz after ~0.4 billion years due to radiation losses. Such a source could have a flux density of 400 Jy at 3 MHz (easily detected by a LFSA) and yet be < 2 mJy at 1.4 GHz, below the

detection limit of even the recent VLA Sky Survey (Condon, et al. 1998). However, some theorists have questioned the interpretation of radio galaxy spectra in terms of synchrotron aging (Rudnick et al. 1994). This issue can only be resolved by low frequency observations.

High redshift radio galaxies

A LFSA will expand the number of known galaxies at the highest redshifts. Extragalactic sources with steep spectra at low frequencies are typically high-z galaxies (e.g., Krolik and Chen 1991). A LFSA is well suited to select the steepest-spectrum sources from, for example, the 6C catalog at 151 MHz (Blundell et al. 1998), which are expected to be the most distant ones ($z > 4$). This distance limit increases with decreasing survey frequency, and consequently a low frequency sky survey will provide a glimpse of the Universe at a time when galaxies were young, possibly back to the protogalaxy era (Silk and Rees 1998).

Cosmic ray distributions in other galaxies

A LFSA will map the low frequency surface brightness distributions in nearby galaxies. This will provide information on the distribution and evolution of low energy cosmic ray electrons, such as their diffusion time away from the galactic disk (and thus the strength of the interstellar magnetic field) and the extent of the cosmic ray halo (e.g., Perley and Erickson 1979; Winter, et al. 1980). The extent and spectra of nonthermal radiation provide information on past star formation in other galaxies (e.g., Lisenfeld, et al. 1998).

1.2.3 Understand the life cycles of matter in the universe

The interstellar medium is the component of the Galaxy from which stars form, to which massive stars return chemically enriched material, and through which matter and energy are exchanged between stars. Understanding the physical conditions in the interstellar medium is critical to understanding galactic evolution.

Distribution of diffuse ionized hydrogen

Ionized hydrogen is "the only major component of the interstellar medium that has not yet been surveyed" (Reynolds 1990). It is important to determine the large-scale distribution of diffuse HII both to improve our understanding of the heating and ionization processes in the interstellar medium and to account for the emission or absorption by this gas in other parts of the spectrum. A LFSA *will determine the galactic distribution of diffuse HII by measuring the free-free absorption of radiation along the lines of sight to a large number of bright galactic and extragalactic sources* (e.g., Kassim 1989). Free-free absorption due to intervening ionized hydrogen produces a more steeply inverted spectrum below the turnover frequency than synchrotron self-absorption or internal free-free absorption, and thus the processes can be distinguished (see Figure 4).

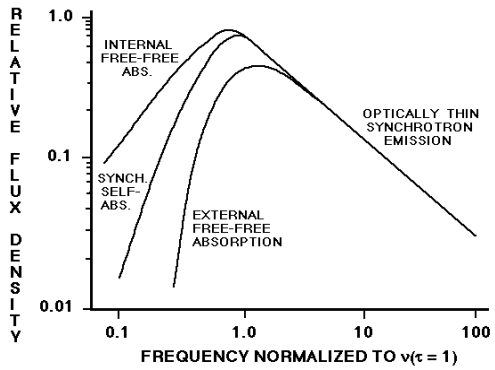

Figure 4 — The spectral signatures of low frequency absorption processes.

These measurements by a LFSA will cover high galactic latitudes and can be combined with pulsar dispersion measures at low galactic latitudes and with recent Hα surveys.

Plasma turbulence in the Galaxy

A better understanding of all aspects of interstellar scattering will tell us more about the turbulence properties of the interstellar plasma (energy input and transport) and consequently will shed light on its role in star formation and galactic evolution. A LFSA can contribute to this goal in several ways. A LFSA *will be able to map the distribution of scattering material by measuring the angular broadening of distant sources in all directions* (e.g., Taylor and Cordes 1993), including high galactic latitudes.

For paths which pass only through the diffuse "type A" interstellar scattering medium (Cordes, Weisberg & Boriakoff, 1985), it will be possible to directly measure the inner scale of the turbulence. This is not possible with ground-based VLBI arrays operating at higher frequencies because the scattering disk is too small at these frequencies to resolve with Earth baselines. Only scattering by the clumpy "type B" component of the interstellar medium is observable with ground-based VLBI. *A LFSA's determination of the inner scale for type A scattering will help identify the physical properties of the plasma responsible, and thus help understand heating of the diffuse interstellar medium by turbulent energy dissipation.*

Another interesting observation will be the angular sizes of extragalactic sources which display low frequency (meaning hundreds of MHz in this case) variability in flux density. This variability is usually attributed to refractive interstellar scintillation (Rickett, Coles, & Bourgois 1984). A definitive test of this hypothesis will be possible by comparing the diffractive angular sizes measured by a LFSA (and scaled to frequencies where flux density variations are observed) with the intrinsic angular sizes determined by VLBI at high frequencies. The refractive scintillation model requires the diffractive scattering disk and the intrinsic angular size to be similar (Rickett, 1986).

Origin of cosmic ray electrons

A LFSA will test the hypothesis that cosmic ray electrons originate in galactic supernova remnants by *directly detecting the presence of low energy electrons needed to initiate shock acceleration mechanisms.* In addition, comparison of low and high frequency images of supernova remnants will allow spectral variations to be mapped, providing information on locations and efficiency of shock acceleration.

Galactic low energy cosmic ray distribution

Low frequency radio observations with sufficient angular resolution to resolve dense HII regions offer the only way to measure the space distribution of cosmic ray electrons with energies < 1 GeV. A LFSA *will determine the volume emissivity distribution in our Galaxy by measuring the emission from lines of sight to nearby opaque HII regions.* If the distance to the HII region and its electron temperature are known the nonthermal emission per unit path length can be found (Kassim 1990). Measurements of synchrotron emissivity in the 1-30 MHz region will directly give the density of low energy cosmic ray electrons.

1.2.4 Discovery of new phenomena and tests of physical theories

Many physical processes involved in the emission and absorption of radiation are only observable at low radio frequencies. These include various coherent emission processes, plasma (free-free) absorption, synchrotron self-absorption in extended sources, and low frequency spectral cutoffs caused by cutoffs in electron energy distributions. Each of these processes provides unique information on the conditions in distant plasma environments.

New sources of coherent radio emission

A LFSA will detect coherent radio emission from a wide range of objects by measuring their low frequency spectra and variability. Coherent emission processes, capable of producing extremely high brightness temperature radio emission, are common at long wavelengths. The Sun, giant planets and Earth's magnetosphere all display extremely strong coherent emission at low radio frequencies, and basic physics predicts that similar processes will produce strong low frequency radio emission from objects such as supernova remnants, active galaxies, and quasars.

At present, pulsars and circumstellar masers are the only objects outside our solar system which are known to radiate coherently. At frequencies of a few MHz, however, many of the most intense discrete galactic sources in the sky (outside of the solar system) will be coherently-emitting sources driven by accretion and outflow. These are objects at the extremes of stellar evolution, with protostellar systems on one end and binary white dwarfs and neutron stars on the other. Emission associated with electron cyclotron masers, as seen from the giant planets, Earth (Auroral Kilometric Radiation), and several nearby stars, *is not only expected to occur and be detectable elsewhere in the Galaxy, but to be ubiquitous.*

Figure 5 shows the time-averaged radio burst emission from Jupiter as a function of frequency from single-spacecraft observations. Below about 10 MHz electron-cyclotron maser emission is <u>many orders of magnitude</u> more intense than the incoherent synchrotron emission at higher frequencies. This type of emission (and the information it contains on local plasma and gyro frequencies) can <u>only</u> be detected and studied at low frequencies.

Pulsars whose radio spectra have no observed low-frequency turnover, such as the Crab pulsar and some millisecond pulsars, are promising targets. These pulsars will be among the strongest sources in the sky at frequencies below about 10 MHz (e.g., Erickson and Mahoney 1985). Timing data at higher frequencies provide an upper limit on the size of the coherent emitting region (Phillips & Wolszczan 1990) while measurement of a low-frequency spectral turnover by a LFSA will provide a lower limit. In this way a LFSA will probe one of the most extreme environments known.

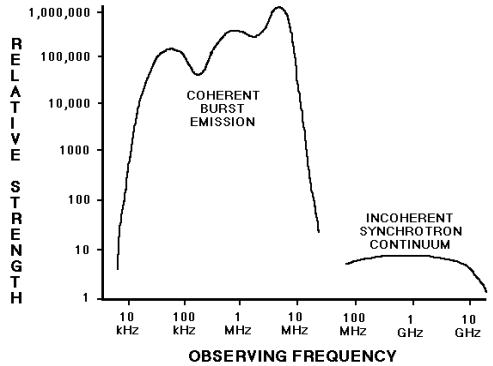

Figure 5 — Time-averaged radio emission from Jupiter. The peak burst intensities are an additional two orders of magnitude higher than shown (figure adapted from Carr, Desch, and Alexander 1984).

In addition, a large increase in low frequency radio brightness is expected from coherent emission in relativistic jets (e.g., Baker et al. 1988; Benford 1992). This will allow a much larger number of extragalactic objects to be detected than would otherwise be possible. The best way to identify coherent emission from objects outside the solar system will be based on their spectra (see Figure 5).

Shock acceleration in supernova remnants

A LFSA will measure the distribution of spectral shape throughout supernova remnants, thereby identifying the sites where shock acceleration begins. Diffusive shock acceleration in supernova remnants has long been thought to produce the observed high

energy cosmic rays. However, the spectrum of cosmic ray electrons differs from that of the ions, and this may indicate a different origin for the electrons. Furthermore, it is difficult for thermal electrons to gain enough momentum (compared to thermal ions) to respond to diffusive shock acceleration. *Only observations by a LFSA at low frequencies can detect (via their synchrotron emission) the presence of the relatively low energy electrons which need to be available for injection into the diffusive shock acceleration mechanism.* X-ray images detect synchrotron radiation from very high energy electrons in supernova remnants (Koyama et al. 1995), but are insensitive to low energy electrons.

Possible new non-thermal galactic sources

A LFSA will image galactic supernova remnants and other extended structures to search for new non-thermal emission (e.g., Erickson and Perley 1975). For example, the question of whether the Crab nebula is located inside a previously undetected fast shock, as expected from mass and energy considerations, is still unresolved (Frail, et al. 1995; Sankrit and Hester 1997; Jones, et al. 1998). Because of its relatively steep spectrum, emission from the blast wave will be most easily seen at low frequencies. For the same reason, nonthermal emission associated with galactic features such as HI supershells (possibly remnants of previous γ-ray bursts; Loeb & Perna 1998; Efremov et al. 1998), very old supernova remnants, the galactic center fountain, and large-scale ionized filaments (Haffner et al. 1998) will likely be found at low frequencies. Such emission contains information on the location and strength of shocks, and can allow very extended (old) remnants to be detected. A more complete sample of old explosive remnants provided by a LFSA is essential to improve estimates of the frequency of supernovae and γ-ray bursts in our Galaxy and the total kinetic energy input to the interstellar medium from explosive events.

Diffuse emission from galaxy clusters

A LFSA will accurately measure the low frequency spectrum and angular size of halo radio emission in clusters of galaxies, and thereby test the hypothesis that some of the observed X-ray and extreme UV emission coming from the intracluster gas is due to inverse-Compton scattering of microwave background photons by the low-energy electrons producing the synchrotron emission that is strongest in the low frequency range (Henning 1989; Sarazin and Lieu 1998). This will tell us how much of the observed X-ray emission is produced by thermal bremsstrahlung from diffuse gas in the cluster, and consequently the true density and temperature of the thermal gas. The origin and maintenance of cluster radio halos are open questions. A LFSA will distinguish between leakage from galaxies and particle interactions as the origin of relativistic electrons in cluster halos.

Scattering by charged dusty plasmas

Dusty plasma effects are of great interest for any astrophysical environment where dust is a significant component, such as interstellar dust clouds and regions of star and planet formation. A LFSA *will test the hypothesis that radiation at long wavelengths can interact with charged dust in a quasi-coherent manner to produce enhanced scattering (Ginzburg and Tsytovich 1990) by measuring the intensity of scattered solar radiation as a function of frequency and height in the corona.* A cloud of shielding ions or electrons surrounds electrically charged dust particles and has dimensions on the order of the Debye length, which is 1-10 meters in the solar corona. Wavelengths longer than the Debye length should be strongly scattered by coherent oscillations of the entire Debye

cloud. Low frequencies are ideal to detect the predicted enhanced scattering of radio waves longer than the Debye length and coupling between the dust and moving plasma in the solar wind.

Extrasolar Planet Detection

A LFSA will search for radio emission from Jupiter-like planets orbiting nearby stars. The radio emission from Jupiter itself would be well below the detection limits of a LFSA at the distance of even the nearest stars. However, there are reasons to expect that low frequency radio emission from a giant planet in a newly formed solar system, orbiting a giant star, or in a planetary nebula, could exceed that of Jupiter by many orders of magnitude. This could occur because emission by stellar-wind-driven cyclotron masers is a very strong function of the stellar wind energy flux (Farrell et al. 1998; see Figure 6), which will be much larger in some systems than in our solar system.

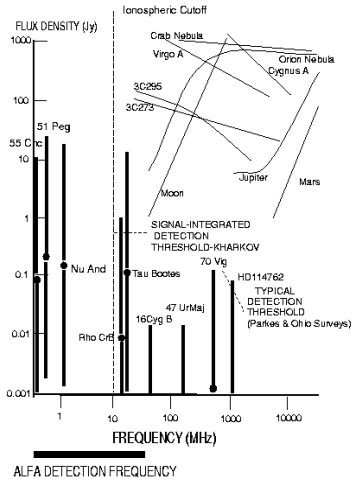

Figure 6 — Coherent cyclotron power and freq. expected from known extrasolar planets.

Also, a recently formed gas giant planet may have a stronger magnetic field, and therefore a larger magnetosphere, than Jupiter. Thus *it may be possible to detect low frequency radio emission from extrasolar planets with a LFSA.*

1.3 SOLAR/SPACE PHYSICS

With a LFSA we propose to take the next logical and long overdue step in solar radio astronomy from space, namely to image the sun at low frequencies. Only at low frequencies can solar transient phenomena such as coronal mass ejections be imaged in detail and tracked from 2 R_{SUN} out to the vicinity of Earth. These observations can only be made from space. A LFSA will address fundamental solar/space physics issues of solar variability, terrestrial response, and space weather forecasting.

1.3.1 Introduction

The study of the nature & evolution of solar transient phenomena is essential to understanding the sun-Earth connection. Phenomena such as solar flares, filament eruptions, fast mode shocks, and coronal mass ejections (CMEs) are manifested by distinct types of non-thermal radio bursts. A LFSA will image these radio bursts at low frequencies to reveal their spatial and temporal evolution, and to permit remote sensing of coronal and interplanetary density and magnetic field structures between the sun and Earth. Images of transient radio bursts are also very important for space weather forecasting.

Transient disturbances traveling through interplanetary space generate radio emissions at the characteristic frequencies of the plasma.

Type II radio bursts are generated by shocks from flares and/or CMEs, *type III* radio bursts are produced by suprathermal electron beams usually associated with solar flares, and *moving type IV* radio bursts are generated by ejected plasma from filament eruptions. The radio frequencies associated with the evolution of solar disturbances range from a few kilohertz to several gigahertz, decreasing with the height of the disturbance in the solar atmosphere. The higher frequency emissions occur very close to the sun where the electron density and plasma frequencies are high, while lower frequency emission occurs in the less dense regions far from the sun. Ground-based radio observations are limited by Earth's ionosphere to frequencies above 20-30 MHz and therefore to solar emissions that are generated close to the sun (<2 R_S). For the vast spatial region between the sun and Earth, radio observations from space provide a proven way to observe transients in the sun's extended atmosphere. There have been numerous space-based radio instruments that have made and continue to make low-frequency observations of the sun. However, without exception, these observations are made with simple dipole antennas from single spacecraft and provide very poor angular resolution. Even the proposed STEREO mission will only use dipole antennas and will only be able to track the centroids of radio bursts.

In addition to nonthermal emission, some of these disturbances are also sources of thermal radio emission**.** Low frequency images of thermal emission will, for the first time, provide information on coronal hole, streamer, and CME structures at heliocentric distances greater than 2 solar radii — thereby complementing and significantly extending maps of these structures obtained by white light and X-ray imaging.

The important solar-terrestrial physics goals of a LFSA are:

- Image and track the transport of CMEs in the interplanetary medium to improve understanding of their evolution and propagation, to distinguish unambiguously between Earth-directed and anti-Earth-directed CMEs, to establish a metric for their "geoeffectiveness", and to predict their Earth arrival times for space weather forecasting purposes.
- Map the large-scale interplanetary magnetic field topology and interplanetary density structures, such as coronal streamers, coronal holes, and the heliospheric current sheet, to improve and extend existing coronal and solar wind models of the inner heliosphere.
- Enhance understanding of particle acceleration in flares and in shocks driven by CMEs and provide new insights into the radio emission mechanisms.
- Provide global imaging of the terrestrial magnetosphere to better understand the response of the magnetosphere to the impact of major events such as CMEs.
- Apply solar results to better understand stellar radio sources such as flare stars.

The realization of these solar-terrestrial science goals will open up whole new vistas in low-frequency solar physics and will inevitably lead to the discovery of new solar processes in addition to those anticipated in this proposal.

1.3.2 Low-Frequency Imaging

Ground-based radio telescopes have had the capability for nearly three decades to image solar emissions using the technique of aperture synthesis. The top image in Figure 7 (Gopalswamy et al. 1987) shows an example of radio isointensity contours from solar thermal emissions with a superposed non-thermal type III source to the southeast, as observed by Clark Lake at 50 MHz. Because

Earth's ionosphere hinders observations at frequencies below about 30 MHz (height above sun >0.5 R_S), tracking solar disturbances from the sun to the vicinity of Earth is the domain of *space-based radio observations.*

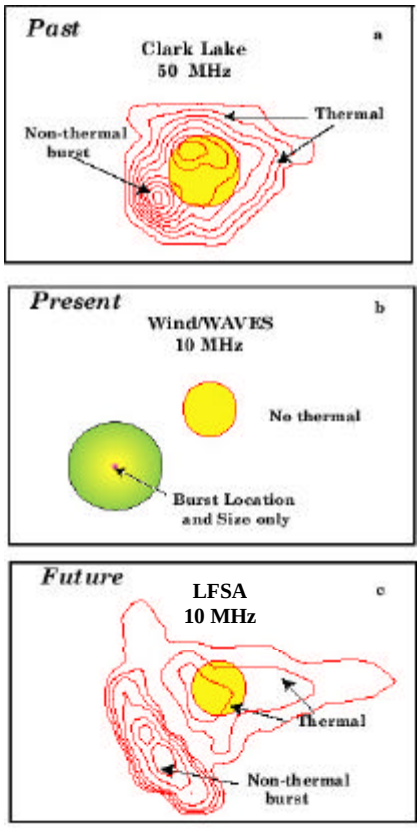

Figure 7 — Improved imaging of both non-thermal and thermal radio emission from the sun (yellow) by a LFSA.

The middle part of Figure 7 shows what the current state-of-the-art WAVES experiment on the Wind spacecraft would have observed at 10 MHz from the type III radio burst shown in the top panel. (WAVES cannot detect the solar thermal emissions.) The WAVES instrument could determine the centroid of the nonthermal emission region and obtain an estimate of the overall size (e.g. Manning and Fainberg 1980), but detailed spatial information could not be obtained. The proposed STEREO mission will produce similar measurements from two vantage points, with no imaging capability.

In the lower part of Figure 7, we show the expected image of the thermal and non-thermal radio sources at 10 MHz which could be obtained by a LFSA. Because of the extended dynamic range of a LFSA it will be possible to image both thermal and non-thermal sources simultaneously. A LFSA will extend these observations well into the interplanetary medium (to nearly 200 R_{SUN}) by providing the first low-frequency, high-angular-resolution radio images associated with solar transient disturbances. Unlike ground-based scintillation monitoring of inter-planetary density enhancements, a LFSA will provide both high temporal and high spatial resolution.

The radio images produced by a LFSA will let us track the interplanetary transport of coronal mass ejections, map the large-scale three dimensional structure of interplanetary magnetic fields, map both transient and quasi-stable density structures, and discover mechanisms and sites of energetic particle acceleration.

1.3.3 Imaging of the Quiet Sun

In the outer corona (>2 R_S) the solar magnetic field is predominantly open and the quiet sun structure is relatively simple, containing coronal holes and streamers. Images of the quiet corona were made down to about 26 MHz, close to the ionospheric cutoff, by ground based arrays such as the Clark Lake radioheliograph. The quiet sun emission is thermal bremsstrahlung from the 10^6 K coronal plasma. *A LFSA will image the quiet corona to unprecedented heliocentric distances.*

Coronal streamers on the solar disk overlie dark filaments and constitute the pre-eruption state of a CME. The coronal holes on the solar disk are sources of fast solar wind

streams. Monitoring these coronal structures at low frequencies is valuable because they constitute important sources of disturbances that influence Earth. A LFSA will image these coronal streamers and coronal holes as enhancements and depressions with respect to the quiet corona. A LFSA will not be faced with the problem of ionospheric effects such as acoustogravity waves and so we can precisely determine the location of the coronal holes and streamers against the solar disk at distances significantly larger than those obtained from X-ray images. The origin and initial extent of Earth-directed CMEs can be estimated from the structural changes in the streamers. Since the CME is a moving density enhancement with respect to the ambient corona, it will also produce enhanced bremsstrahlung emission.

1.3.4 Shock Waves & Interplanetary CME Transport

A LFSA will image and track CME-driven shocks by observing type II radio bursts generated by shock-accelerated electrons.

Meter wavelength type II bursts have been observed in the solar corona by ground-based observatories since the 1950s, and are associated with coronal shocks. However, kilometric wavelength type II bursts, which are generated by CME-driven shocks propagating through the interplanetary medium, are observed only by sensitive low-frequency spacecraft radio receivers. These interplanetary type II bursts are associated with the fastest shocks, and the radio emission regions can be very large (Lengyel-Frey and Stone 1989). Reiner et al. (1998a,b) demonstrated that kilometric type II emissions originate in the upstream regions of CME-driven shocks. As the CME propagates, different regions of the shock front become the site of radio emissions and therefore the site of particle acceleration. The type II radio emission mechanism depends on the local plasma density, so type II burst observations provide information on plasma density in the vicinity of the shock. Images of kilometric type II bursts obtained by a LFSA, at different frequencies, will therefore provide the first high resolution maps indicating the range of densities in the upstream region of CME-driven shocks, and will provide new information about the sites of particle acceleration along the shock front.

In addition to the radio emission profile associated with the CME-driven shock, the density profile of a transient CME can be indirectly mapped and tracked outward from the sun by imaging behind-the-limb type III bursts. Several investigators (Dulk et al. 1985; Reiner & Stone 1990) have found that intense type III radio emission generated on one side of the sun is often visible from the opposite side. These behind-the-limb bursts are visible due to the scattering of radiation by plasma surrounding the sun. Because of the high speed of type III radio bursts, these behind-the-limb sources illuminate the coronal and interplanetary density configuration from behind nearly instantaneously. By observing at different frequencies, "snapshots" of the density profile of transient coronal structures in the interplanetary medium will be obtained (see Figure 8).

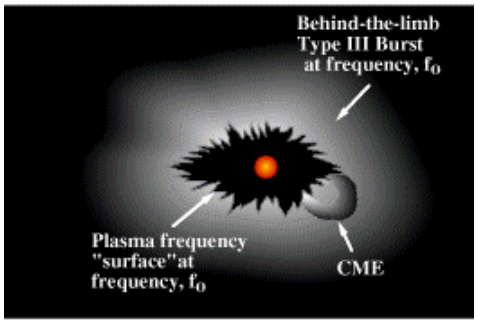

Figure 8 — Tracking a CME using behind-the-sun type III radio bursts.

This method of mapping and tracking will

work best during solar maximum when there can be tens of intense kilometric type III radio bursts per day. During the 3-4 days required for a CME to travel from the sun to 1 AU there will be many behind-the-limb bursts. *This indirect method of mapping and tracking can be applied when the CME is far from the sun where white-light coronagraphic imaging is not possible.* Furthermore, this method accurately measures the density profile in the CME since the density is precisely given by the observed frequency — no assumptions are needed about column density between source and observer.

An exciting possibility with a LFSA will involve applying both the direct and indirect mapping techniques to the same transient CME. The indirect technique provides a near instantaneous density profile of the CME while the direct mapping technique provides the location of radio emission regions at the same time.

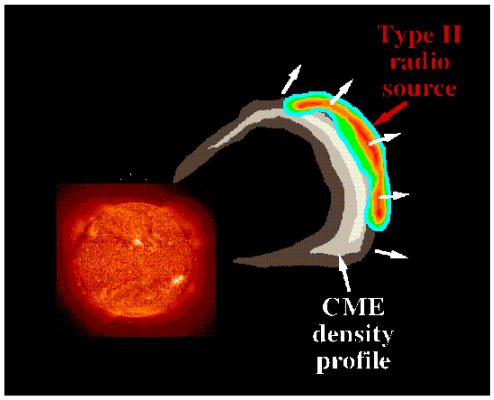

Figure 9 — Simultaneous imaging of CME density profile and shock front.

As illustrated in Figure 9, this will provide the first large-scale picture of where the CME-driven shock lies relative to the CME piston material as it propagates through the inter-planetary medium. Since both the density profile and radio emissions will be measured by the same instrument, ambiguities and difficulties involved in comparing radio and white-light images are removed.

1.3.5 Mapping of Interplanetary Density Structures and Magnetic Field Topology

Only a few observations have permitted direct or remote measurements of density structures and transient disturbances in the inner heliosphere (< 1 AU from the Sun) — *in-situ* measurements by spacecraft such as Helios 1 & 2, interplanetary scintillation observations, and remote tracking of radio bursts by single spacecraft. *The imaging capabilities of a LFSA offer several new methods of mapping density and magnetic field structure in the inner heliosphere.* These new observations will provide a better understanding of the propagation of interplanetary disturbances and the evolution of quasi-stable density and magnetic field structures. They will provide a framework in which interplanetary transients can be interpreted, without relying on models based on long-term averages or widely spaced observations obtained *in situ.*

A LFSA will map the interplanetary density structures inside 1 AU by the direct and indirect imaging techniques described above. A LFSA will obtain, for the first time, frequent high resolution 2-D images of interplanetary type III radio sources, including behind-the-limb type III events and kilometric type III radio storms. By combining images at different frequencies we will construct snapshots of density structures, such as extensions of coronal streamers and the heliospheric current sheet, throughout the inner heliosphere. During the active phase of the solar cycle type III radio bursts occur frequently and many such snapshots will be combined to follow the evolution of these structures.

Both individual type III bursts and type III storms have been used to map the magnetic field topology in the interplanetary medium from single or two-spacecraft observations

(Bougeret et al. 1984; Reiner et al. 1998c). With LFSA images it will be possible to observe both the large-scale structure of the field lines in two dimensions and smaller scale variations due to transients in the solar wind. Since the electrons producing type III bursts follow magnetic field lines outward from their source in the corona, the images of the radio burst also reveal the ensemble of field lines along which the electrons travel. In addition, the draping of magnetic field lines around CMEs, never directly observed (McComas et al. 1989; Reiner et al. 1995), will be evident in these maps. *The ability to map density and magnetic field structures in 2 dimensions, never before possible with high spatial and temporal resolution, will provide a completely new perspective on the interplanetary medium.*

1.3.6 The Terrestrial Response

The primary "geoeffective" disturbances that originate from the sun are: fast solar wind streams, prominence eruptions, and coronal mass ejections (CMEs). The fast wind streams emanate from coronal holes and produce recurring geomagnetic storms with a 27-day periodicity. The non-recurring (and currently unpredictable) geomagnetic storms are caused by CMEs, which pose the greatest danger to ground-based and space-borne technological systems and to astronauts. Space weather involves two basic and important problems: first, predicting, well in advance, when a disturbance will arrive at Earth and, secondly, predicting the geoeffectiveness of a disturbance.

It is well known that CMEs that drive shocks are more geoeffective than those that do not. On the other hand only those CMEs that drive shocks produce type II radio emissions. *Thus, CMEs with associated type II radio emissions are more geoeffective than those that produce no radio signature.* By tracking type II radio bursts, we are selecting CMEs that can cause a significant geomagnetic response, especially during extended periods of southward interplanetary magnetic field orientation.

Connections between solar and terrestrial events have been studied almost exclusively by assuming a propagation velocity from the sun to Earth. It is, however, very difficult to determine the speed and therefore the transit time of a disturbance from observations made near the sun. Furthermore, speeds observed near the sun can be significantly different from the speed of propagation in the interplanetary medium. As a result, a predicted Earth arrival time based on coronagraph images can be in error by a day or two. Clearly, what is keenly needed is a means of tracking the solar disturbance through interplanetary space. *The tracking of CMEs by a LFSA will provide a key link in the solar-terrestrial relationship.* With a LFSA the accuracy and timeliness of predictions will be significantly improved over what is currently possible using type II burst data from the Wind spacecraft. Type II burst images constructed in near-real-time by a LFSA will enable accurate (to within hours) predictions to be made, days prior to a CME arrival at Earth.

1.3.7 The Terrestrial Magnetosphere

A low frequency array will probably be in an orbit quite distant from Earth, providing an ideal opportunity to image Earth's magneto-sphere and bow shock from many vantage

points over the array lifetime. At frequencies below a few hundred kHz, Earth's naturally-occurring radio emissions — the Auroral Kilometric Radiation (AKR), trapped continuum, and emission at twice the *in-situ* plasma frequency (2fp) — will delineate regions of near-Earth space with strong gradients in the plasma and magnetic fields. At Earth's bow shock, 2fp emission is generated nearly continuously by electrons backstreaming along interplanetary magnetic field (IMF) lines tangent to the bow shock (Reiner et al. 1997). Since the IMF is constantly changing orientation and hence its contact point, imaging of the source region will trace a locus of points just upstream of the bow shock surface.

Deeper within the magnetosphere, the AKR and trapped continuum are scattered by density irregularities in the dayside cusp, magneto-sheath, and magnetotail, essentially "lighting up" the entire magnetosphere (e.g., Figure 10; Alexander and Kaiser 1977).

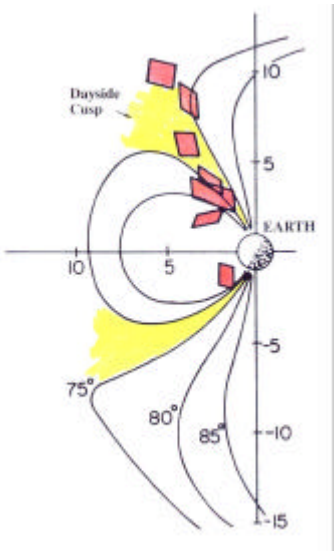

Figure 10 — Magnetospheric emission (AKR) near 200 kHz scattered off of density irregularities. This defines the day-side cusp; a LFSA will provide frequent imaging of such magnetospheric structures.

While the AKR and continuum are quasi-continuous sources of emission, a distinct component of the AKR is now known to occur only with southward turnings of the IMF (Desch 1996) and the onset of magnetic substorms (Anderson et al. 1996). A LFSA *will produce high signal-to-noise images of the terrestrial magnetosphere precisely when the most interesting solar wind-magnetosphere interactions, such as magnetic reconnection, are taking place.*

At the distance of a LFSA of ~160 R_E from Earth, the frontside magnetosphere will subtend 21° and the magnetotail will extend over 40° (Alexander et al. 1979). Bow shock and magnetospheric emissions, while occurring simultaneously, are well separated in frequency and therefore will constitute distinct radio images. Imaging is possible not only on a routine basis but especially when reconnection is occurring on the frontside. *These will be the first images of a planetary magneto-sphere from the outside and likely the only global images produced during active periods.*

2. INSTRUMENTAL CONCEPT

Obtaining the desired data with a LFSA will present no major technical challenges. Data analysis, however, will require both efficient algorithms for very-wide-field imaging and a significant computing capability. However, it appears that there are no fundamental problems with full-sky imaging by a spherical aperture synthesis array, that issues of source variability and terrestrial radio interference have been successfully solved, and that the computing resources needed for data analysis are available and affordable.

2.1 INSTRUMENTATION

A conceptual LFSA array might consist of sixteen satellites operating together as an interferometer. Low frequency radio radiation will be sampled by a pair of orthogonal dipole antennas on each of the identical satellites, and each dipole will feed signals to a simple but flexible high dynamic range receiver. Observing frequency, band-width, sample rate, and phase switching are controlled by a central spacecraft processor, and can be changed at will. A block diagram of a receiver is shown in Figure 11.

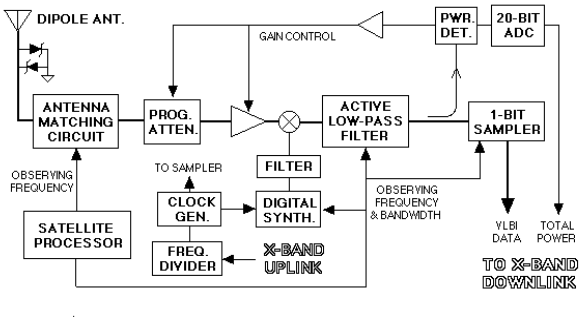

Figure 11 — Low frequency receiver.

The receiver design is based on commercially available components. It covers 0.03-30.0 MHz, with Nyquist sampled bandwidths up to 125 kHz and an ability to handle a very wide range of input levels. No new development is required.

2.2 ARRAY

A LFSA will have a maximum baseline length of ~100 km, which provides a good over-all match to interstellar and interplanetary angular broadening. The array may be placed in a well understood, nearly circular distant retrograde orbit (DRO) about the Earth-Moon barycenter, with a typical distance from Earth of one million km where the dynamics of the array are presently solvable. There are many advantages of a DRO for this array, including sufficient distance from Earth to minimize terrestrial interference combined with the ability of each satellite to communicate directly with relatively small (11-meter) and affordable ground stations. Note that this concept involves no reliance on a single spacecraft for data relay or any other array critical function; the array data path is extremely robust (16-way redundancy) all the way to the ground. Similarly robust is our technique for continuously monitoring the relative positions of the satellites by measuring the separations between all pairs of satellites. This provides far more constraints than are needed to solve for all of the relative positions. Should one or more of the array satellites fail, observing by the rest of the array continues unhampered.

Each satellite receives an X-band carrier (to which the local oscillators are phase locked) and low-rate command telemetry, and

transmits X-band data to the ground continuously at 0.5 Mb/s per satellite. The distance of the DRO and its location in the ecliptic plane allows continuous coverage of the array by three ground stations. At the ground station telemetry headers are removed and the remaining interferometry data from each satellite are recorded on tapes for transport to the correlation computer. Small subsets of the data for rapid solar snapshot imaging will also be stored on disk and retrieved from the stations via internet. The DSN 11-m ground stations are currently operational, and operator intervention would be required only for occasional (once every several days) tape changes or in case of station equipment failure.

2.3 DATA ANALYSIS AND ARCHIVING

2.3.1 Array Configuration

Among the challenges of imaging the sky at low radio frequencies is the need to image the entire sky at the same time. This is necessary because individual radio antennas of reasonable size have very low directivity at these wavelengths (which is the motivation for using an interferometer array in the first place). Consequently very strong radio sources will create sidelobes in directions far from their positions, and high dynamic range imaging will require that the effects of strong sources be removed from all sky directions, not just from the region immediately adjacent to the sources. This in turn requires an array geometry which produces highly uniform aperture plane coverage in all directions simultaneously, a requirement that no previous interferometer array has had to meet.

A quasi-random distribution of antennas on a single spherical surface has been found to provide excellent aperture plane coverage in all directions with a minimum number of antennas. This concept was developed by Steve Unwin at Caltech, who noted the importance of using a minimum separation constraint when computing antenna locations to avoid an excessive number of short projected spacings. We will refer to this type of configuration as an "Unwin sphere". An example of the aperture plane (u,v) coverage provided by a 16-antenna Unwin sphere is shown in Figs. 12 & 13.

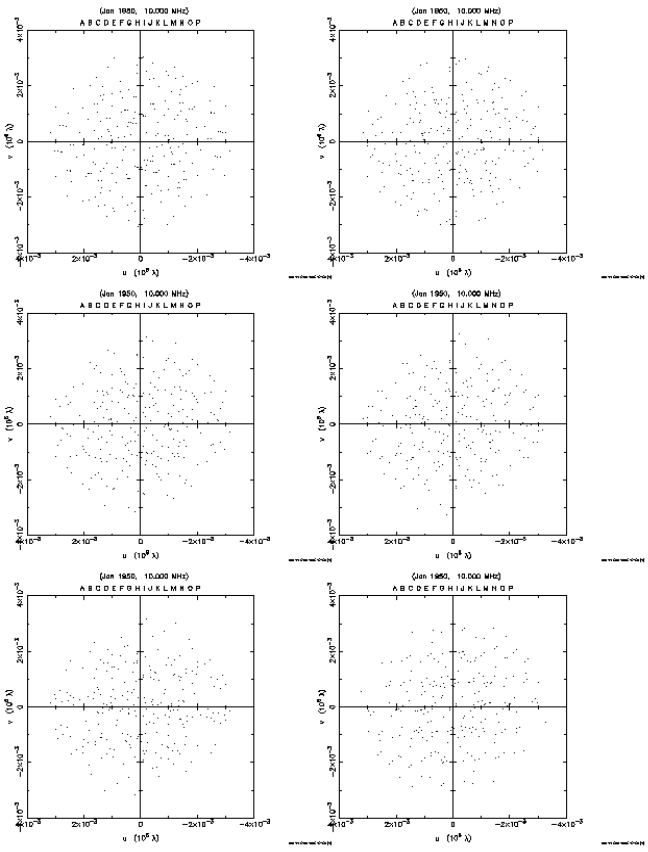

Figure 1: Array 15sn2 – (u,v) coverage for 0, 12, 24, 37, 53, and 90deg ecliptic latitude.

Figure 12 — Instantaneous aperture plane sampling in six widely separated directions.

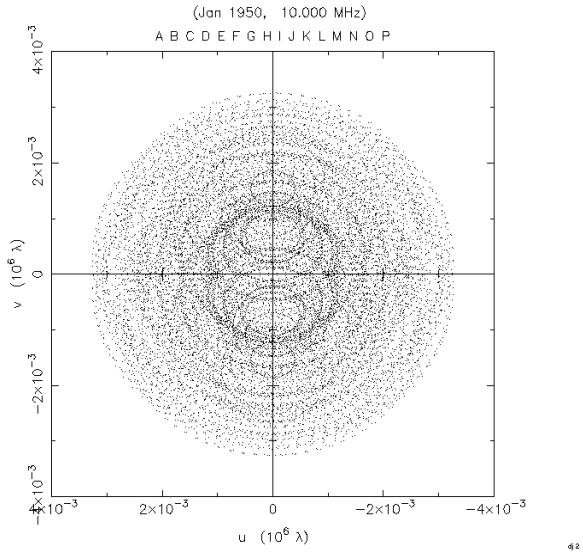

Figure 13 — Long-term (u,v) sampling.

Figure 12 shows the instantaneous projected sampling in six directions covering 0 to 90 degrees in ecliptic latitude. The coverage in each direction is nearly ideal for two dimensional imaging, and indeed is far better than the coverage used to produce snap-shot images with ground-based VLBI.

Figure 13 shows the truly excellent sampling obtained by allowing the Unwin sphere to slowly rotate. The coverage is far more uniform in every direction than that produced in a single direction by any ground-based VLBI array. Note that even over the inner few km the sampling remains highly uniform. These short baseline spacings are important for imaging very extended sources such as type II solar radio bursts and emission from the galactic plane.

The synthesized beam produced by the sampling shown in Figure 13 at an intermediate ecliptic latitude is shown in Figure 14. A Gaussian taper was applied to the visibility data; this weighting scheme sacrifices some angular resolution to obtain lower sidelobe levels. The sidelobes in Figure 14 are generally at or below +/- 1% of the peak, even very close to the main beam. This is a remarkably clean synthesized beam, which will help deconvolution algorithms work well.

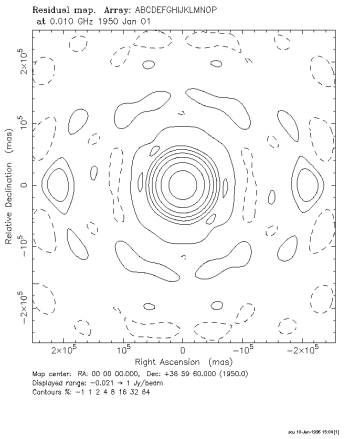

Figure 14 — Synthesized beam.

2.3.2 Cross-correlation

Cross-correlation of the signals will be done by Fourier transforming data from each satellite into a time series of frequency spectra and then cross-multiplying pairs of spectra to obtain the cross-power spectra for each baseline and for each phase center. The computing power required to cross-correlate all data in less than the observing time (3 GFLOPS) can be obtained from a cluster of workstations, for example eight Sun Ultra 60s. This approach offers greater flexibility and less cost than a dedicated hardware correlator, and will benefit from future workstation performance improvements.

2.3.3 Sidelobe Suppression

Prior to cross-multiplication, all spectra will be multiplied by a combination of Gaussian and cosine functions to filter the frequency response of the array. This greatly reduces the delay beam sidelobes (see Figure 15). The interferometer response is reduced below 1% when the geometric delay exceeds 21 μs. For delays greater than 29 μs the interferometer

response falls below 10^{-3}; the maximum geometric delay of the array is about 330 μs.

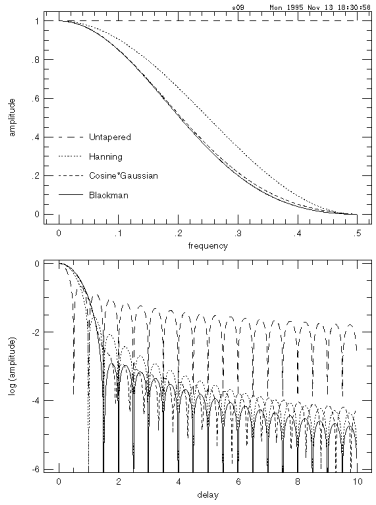

Figure 15 — Bandpass weighting (top) and resulting delay beam (bottom). Dashed line is unweighted and solid line is a preferred weighting.

2.3.4 Interference Suppression

The delay-beam technique for suppressing interferometer response to emission far from the nominal phase center will fail for narrow-band signals. The most obvious source of narrow signals is terrestrial transmitters (see Figure 16). This problem is minimized by a combination of observing frequency selection, a high dynamic range receiver, ionospheric shielding, spectral data editing prior to cross-multiplication, and distance from Earth.

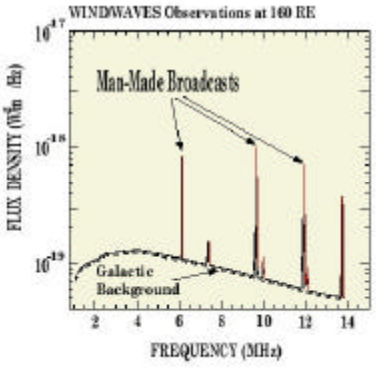

Figure 16 — Terrestrial interference observed by the WAVES instrument on the WIND spacecraft 10^6 km (the conceptual distance of a LFSA) from Earth. At this distance 93% of the measurements above 6 MHz are within 3% of the galactic background. Interference from Earth will not be a serious problem.

2.3.5 Calibration

Phase calibration of the array is provided by the X-band uplink carrier, to which all satellite oscillators are locked. Amplitude calibration is provided by: 1) periodically injecting a known calibration signal into the signal path between the antennas and low frequency receivers, 2) comparison with know astronomical sources at the high end of the LFSA frequency range, and 3) comparison with ground-based observations of solar bursts using antennas of known gain. The measured total power is iteratively divided between the fields of view, starting with the fields containing the strongest sources.

2.3.6 Sensitivity and Dynamic Range

The array sensitivity at 3 MHz is ~20 Jy in 5 minutes. The coherence time limits imposed by fluctuations in the solar wind do not prevent useful imaging even at the lowest frequencies (Linfield 1996). However, it will be confusion noise and dynamic range rather than Galactic background which will limit the number of detectable sources. Confusion effects will be minimized by imaging all strong sources on the sky simultaneously so their flux can be taken into account for each field of view. Dynamic range is determined mainly by the number and distribution of visibility samples, the data signal-to-noise ratio, the quality of calibration, and the complexity of the sources being imaged. Based on our imaging simulations, we expect to obtain a dynamic range of 10^2-10^3 for relatively

compact sources (< 100 beams in size), depending on frequency. For very extended sources or the lowest observing frequencies the dynamic range will still be a few tens, which is entirely adequate for imaging strong, rapidly evolving sources. The use of linearly polarized dipole antennas is not a problem at very low frequencies because radiation will be depolarized by interstellar differential Faraday rotation across any source (Linfield 1995). Interplanetary differential Faraday rotation across the array will also be negligible for solar elongations >90°, even at 1 MHz.

2.3.7 LFSA Imaging Simulations

To verify the very-wide-field imaging performance of a LFSA, we created simulated visibility data for a number of radio sources in different directions and a specified array geometry. These data were combined into a 3-D (u,v,w) visibility data file. Errors applied to the data were calculated from the galactic background plus coherence losses on each baseline predicted by Linfield (1996). As an example of the imaging simulations done, Figure 17 shows the initial (uncleaned) image of a field containing some weak discreet sources. The field is contaminated by sidelobes from a much stronger source 10° to the south.

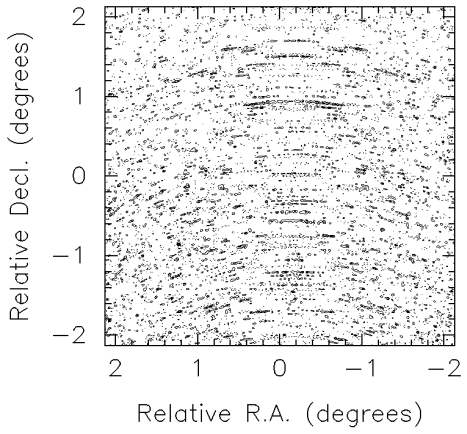

Figure 17 — Initial image of test field.

To improve the dynamic range of the image we first remove the strongest sources in the data set by using only the highest amplitude data points. This allows strong sources to be readily located and modeled. The final image of the strongest source has a dynamic range of ~500, *with no self-calibration.* Once subtraction of the strongest sources has reduced the residual visibility amplitudes to near the expected noise level, the remaining data points are restored and the initial field can be deconvolved. The result is shown in Figure 18. The rms noise level is several hundred times lower than the strongest source in the simulation, and individual sources can now be seen. The final model components contain 99.5% of the total flux density.

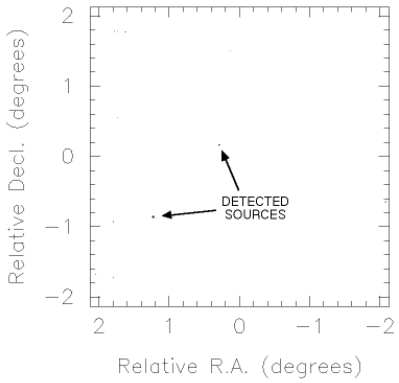

Figure 18 — Deconvolved image of the field in Figure 17, with identical contour levels.

Additional tests were done to verify the ability of this array to image very extended emission such as the galactic plane and angularly large interplanetary transients.

Aperture synthesis imaging of very wide fields requires 3-D Fourier transforms, but regions of limited angular size (over which the effects of sky curvature are small) can be imaged with separate transforms in which one dimension is much smaller than the other two (Cornwell & Perley 1992). This approach

lends itself naturally to parallel processing. For a LFSA the imaging problem is most difficult at the highest frequency (30 MHz) where the synthesized beam is smallest (~20"). We plan to make 4096 x 4096 pixel images with 6 arcsecond pixels, so each image will cover an area of 6.8° x 6.8°. Thus, ~1000 images are needed to cover the entire sky. Each image will require a 16 pixel Fourier transform in the "radial" direction to allow for sky curvature over the largest scale structure to which the data are sensitive. We will divide each image into ~100 smaller areas which will each be deconvolved with the appropriate synthesized or "dirty" beam (*e.g.*, Frail, Kassim, & Weiler 1994). All clean components are subtracted from the data for each field and each field is transformed again to produce residual images. This continues until no sidelobes remain.

3. SUMMARY

In the preceding we have attempted to show that there are many new, exciting areas in astrophysics and solar/space physics which can only be explored by extending our observing capability to radio frequencies below the ionospheric cutoff. This requires going to space, but we have also shown that relatively straightforward concepts exist for a low frequency space array which can open this last unexplored window on the Universe.

References

Alexander, J. K., and Kaiser, M. L., 1977, J. Geophys. Res., 82, 98.

Alexander, J. K., et al., 1979, J. Geophys. Res., 84, 2619.

Anderson, R. R., et al., 1996, Proc. 4th Inter. Workshop on Planetary Radio Emissions, 241.

Bahcall, J., 1991, *Decade of Discovery in Astronomy and Astrophysics* (National Acad. Sci.).

Baker, D. N., Borovsky, J. E., Benford, G., & Eilek, J. A., 1988, Astrophys. J., 326, 110.

Benford, G., 1992, Astrophys. J., 391, L59.

Blundell, K. M., et al., 1998, Mon. Not. Royal Astron. Soc., 295, 265.

Bougeret, J.-L., Fainberg, J., and Stone, R. G., 1984, Astronomy & Astrophys., 136, 255.

Carr, T. D., Desch, M. D., and Alaxender, J. K., 1984, in *Physics of the Jovian Magnetosphere*, ed. A. J. Dessler (Cambridge Univ. Press), 226.

Condon, J. J., et al., 1998, Astronomical J., 115, 1693.

Cordes, J. M., Weisberg, J. M., and Boriakoff, V., 1985, Astrophys. J., 288, 221.

Cordey, R. A., 1987, Mon. Not. Royal Astron. Soc., 227, 695.

Cornwell, T. J., and Perley, R. A., 1992, Astronomy and Astrophysics, 261, 353.

Desch, M. D., 1996, Proc. 4th International Workshop on Planetary Radio Emissions, 251.

Dulk, G. A., Steinberg, J.-L., Lecacheux, A., Hoang, S., and MacDowall, R. J., 1985, Astronomy and Astrophysics, 150, L28.

Efremov, Y. N., Elmegreen, B. G., and Hodge, P. W., 1998, Astrophys. J., 510, L163.

Erickson, W. C., and Mahoney, M. J., 1985, Astrophys. J., 299, L29.

Erickson, W. C., and Perley, R. A., 1975, Astrophys. J., 200, L83.

Farrell, W. M., Desch, M. D., and Zarka, P., 1998, J. Geophys. Res., in press.

Frail, D. A., Kassim, N. E., and Weiler, K. W., 1994, Astronomical J., 107, 1120.

Frail, D. A., Kassim, N. E., Cornwell, T. J., and Goss, W. M., 1995, Astrophys. J., 454, L129.

Ginzburg, V. L., and Tsytovich, V. N., 1990, *Transition Radiation and Transition Scattering* (Bristol and New York: Adam Hilger Publishers).

Gopalswamy, N., Kundu, M. R., and Szabo, A., 1987, Solar Physics, 108, 333.

Goss, W. M., et al., 1987, Mon. Not. Royal Astron. Soc., 226, 979.

Haffner, L. M., Reynolds, R. J., and Tufte, S. L., 1998, Astrophys. J., 501, L83.

Harwit, M., 1984, *Cosmic Discovery* (Cambridge: MIT Press).

Henning, P. A. 1989, Astron. J. 97, 1561.

Jones, T. W., et al., 1998, Publ. Astron. Soc. Pacific, 101, 125.

Kassim, N. E., 1989, Astrophys. J., 347, 915.

Kassim, N. E., 1990, in *Low Frequency Astrophysics from Space* (Lecture Notes in Physics, vol. 362), ed. N. Kassim and K Weiler (Berlin: Springer-Verlag), 144.

Koyama, K., et al., 1995, Nature, 378, 255.

Krolik, J. H., and Chen, W., 1991, Astronomical J., 102, 1659.

Lengyel-Frey, D., and Stone, R. G., 1989, J. Geophys. Res., 94, 159.

Linfield, R. P., 1995, JPL IOM 4-5-95.

Linfield, R. P., 1996, Astronomical J., 111, 2465.

Lisenfeld, U., Alexander, P., Pooley, G. G., and Wilding, T., 1998, Mon. Not. R. Astron. Soc., in press (astro-ph/9805231).

Loeb, A., and Perna, R., 1998, Astrophys. J., 503, L35.

Manning, R., and Fainberg, J., 1980, Space Science Instrum., 5, 161.

McComas, D. J., et al., 1989, J. Geophys. Res., 94, 1465.

Perley, R. A., and Erickson, W. C., 1979, Astrophys. J. Suppl., 41, 131.

Phillips, J. A., and Wolszczan, A., 1990, in *Low Frequency Astrophysics from Space* (Lecture Notes in Physics, vol. 362), ed. N. Kassim and K Weiler (Berlin: Springer-Verlag), 175.

Reiner, M. J., and Stone, R. G., 1990, Solar Physics, 125, 371.

Reiner, M. J., et al., 1995, Space Science Reviews, 72, 261.

Reiner, M. J., et al., 1997, Geophys. Res. Lett., 24, 919.

Reiner, M. J., Kaiser, M. L., Fainberg, J., and Bougeret, J.-L., 1998a, Geophys. Res. Letters, 25, 2493.

Reiner, M. J., Kaiser, M. L., Fainberg, J., Bougeret, J.-L., and Stone, R. G., 1998b, J. Geophys. Res., in press.

Reiner, M. J., Fainberg, J., Kaiser, M. L., and Stone, R. G., 1998c, J. Geophys. Res., 103, 1923.

Reynolds, R. J., 1990, in *Low Frequency Astrophysics from Space* (Lecture Notes in Physics, vol. 362), ed. N. Kassim and K Weiler (Berlin: Springer-Verlag), 121.

Reynolds, C. S., and Begelman, M. C., 1997, Astrophys. J., 487, L135.

Rickett, B. J., 1986, Astrophys. J., 307, 564.

Rickett, B. J., Coles, W. A., and Bourgois, G., 1984, Astronomy & Astrophysics, 134, 390.

Rudnick, L., Katz-Stone, D. M., and Anderson, M. C., 1994, Astrophys. J. Suppl., 90, 955.

Sankrit, R., and Hester, J. J., 1997, Astrophys. J., 491, 796.

Sarazin, C. L., & Lieu, R. 1998, Astrophys. J., 494, L117.

Schmahl, E. J., Gopalswamy, N., and Kundu, M. R., 1994, Solar Phys., 150, 325.

Silk, J., and Rees, M. J., 1998, Astronomy and Astrophysics, 331, L1.

Taylor, J. H., and Cordes, J. M., 1993, Astrophys. J., 411, 674.

Winter, A. J. B., et al., 1980, Mon. Not. Royal Astron. Soc.,